Review

Review of oil spill remote sensing

Merv Fingas [a,*], Carl Brown [b]

[a] Spill Science, Edmonton, Alberta T6W 1J6, Canada
[b] Environmental Science and Technology Section, Environment Canada, Ontario K1A OH3, Canada

ARTICLE INFO

ABSTRACT

Remote-sensing for oil spills is reviewed. The use of visible techniques is ubiquitous, however it gives only the same results as visual monitoring. Oil has no particular spectral features that would allow for identification among the many possible background interferences. Cameras are only useful to provide documentation. In daytime oil absorbs light and remits this as thermal energy at temperatures 3–8 K above ambient, this is detectable by infrared (IR) cameras.

Laser fluorosensors are useful instruments because of their unique capability to identify oil on backgrounds that include water, soil, weeds, ice and snow. They are the only sensor that can positively discriminate oil on most backgrounds. Radar detects oil on water by the fact that oil will dampen water-surface capillary waves under low to moderate wave/wind conditions. Radar offers the only potential for large area searches, day/night and foul weather remote sensing.

© 2014 Elsevier Ltd. All rights reserved.

Contents

* Corresponding author. Tel.: +1 780 9896059.
  E-mail addresses: fingasmerv@shaw.ca (M. Fingas), Carl.Brown@ec.gc.ca (C. Brown).

1. Introduction

Remote sensing is an important part of oil spill response. Public and media scrutiny is usually intense following a large spill, with demands that the location and extent of the oil spill be precisely known. Through the use of modern remote sensing instrumentation, oil can be monitored on the open sea on a 24-h basis (Robbe and Hengstermann, 2006). With the knowledge of slick locations and movement, response personnel can more effectively plan countermeasures to lessen the effects of the pollution. An additional role for remote sensing has been the strong interest in detection of illegal discharges, especially in view of the large seabird mortality associated with such discharges (O'Hara et al., 2013).

The most common forms of oil spill surveillance and mapping are still sometimes carried out with simple still or video photography. Remote sensing from an aircraft (including unmanned aerial vehicles (UAVs), i.e. drones) is still the most common form of oil spill tracking. Remote sensing from satellites using radar sensors is also becoming a common technique. Attempts to use visual satellite remote sensing for oil spills are improving, although success is not necessarily as claimed and is generally limited to identifying features at sites where known oil spills have occurred.

It is important to divide the uses of remote sensing into the end use or objective as the utility of the sensor or sensor system is best defined that way. Oil spill remote sensing systems used for routine surveillance certainly differ from those used to detect oil on shorelines or land. One tool does not serve for all functions. For a given function, many types of systems may, in fact, be needed. Further it is necessary to consider the end use of the data. The end use of the data, be it location of the spill, enforcement or support to cleanup, may also dictate the resolution or character of the data needed.

There are several broad uses of oil spill remote sensing:

1. Mapping of spills.
2. Surveillance and general slick detection.
3. Provision of evidence for prosecution.
4. Enforcement of ship discharge laws.
5. Direction of oil spill countermeasures.
6. Determination of slick trajectories.

Several general reviews of oil spill remote sensing have been prepared (Fingas and Brown, 2011; Leifer et al., 2012; Robbe and Hengstermann, 2006). These reviews generally show that specialized sensors offer advantages compared to off-the-shelf sensors which are usually designed for other purposes.

2. Optical remote sensing

2.1. Optical properties of oil

There are several optical properties of concern to the appearance of oil in the region from the ultraviolet to the near infrared. This includes the reflectance, absorbance and the resulting contrast between oil and water. This, of course changes somewhat with oil type, oil weathering, atmospheric conditions (e.g. fog) and sun illumination. Oil/water differences have not been measured across the spectrum in great accuracy for all conditions and at all wavelengths (Andreou and Karathanassi, 2011; Bulgarelli and Djavidnia, 2012; Kudryashova et al., 1986; Otremba and Piskozub, 2001; Shen et al., 2011; Yin et al., 2012). However a summary can be prepared and is shown in Figs. 1–3. These figures are generalized and do not show sharp features that may be present. The point of these figures is that there does not exist, any broad
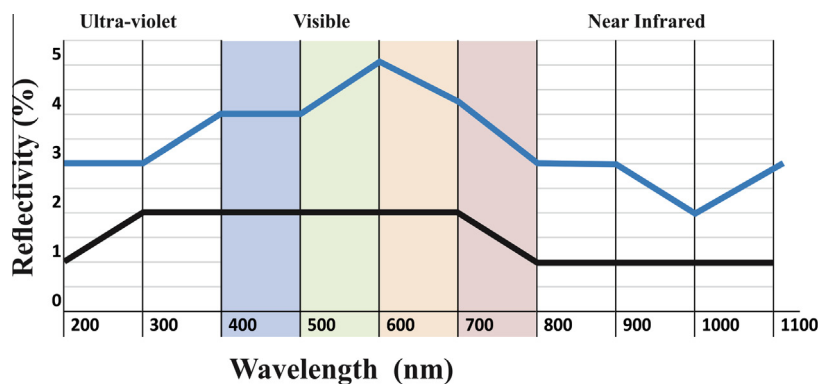
Fig. 1. The generalized vertical reflectance of oil and water. The blue line is the water and the black line the oil. (Generalized from: Andreou and Karathanassi, 2011; Bulgarelli and Djavidnia, 2012; Kudryashova et al., 1986; Otremba and Piskozub, 2001; Shen et al., 2011; Yin et al., 2012). (For interpretation of the references to color in this figure legend, the reader is referred to the web version of this article.)
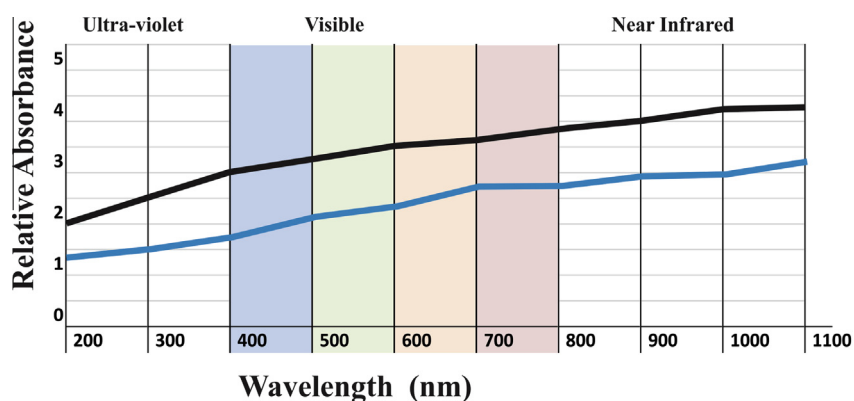

Fig. 2. The hypothetical absorbance of oil and water (Generalized from Kudryashova et al., 1986) The blue line is the water (water-to-air) and the black line the oil (oil-to-air). (For interpretation of the references to color in this figure legend, the reader is referred to the web version of this article.)
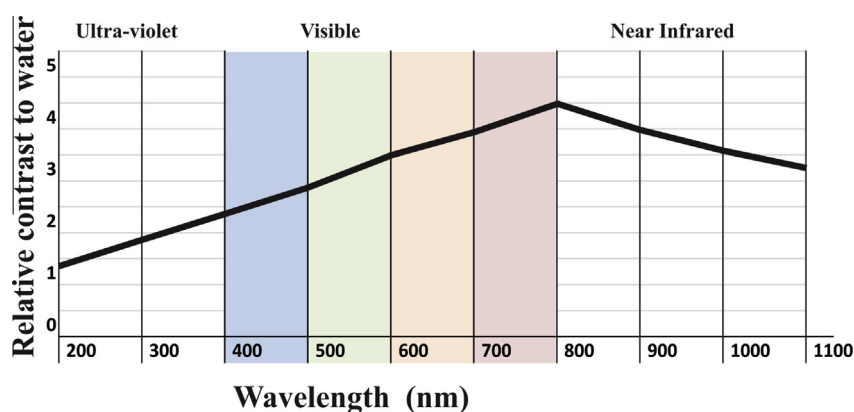
Fig. 3. The hypothetical contrast of oil and water (Generalized from Figs. 1 and 2) The black line the oil as compared to the baseline of water.

distinctions between oil and water in the visible such that one can positively identify oil.

2.2. Visible remote sensing

In the visible region of the electromagnetic spectrum (approximately 400–700 nm), oil has a higher surface reflectance than water, but does not show specific absorption/reflection tendencies. Oil generally manifests throughout the entire visible spectrum. Sheen shows up silvery and reflects light over a wide spectral region down to the blue. As there is no strong information in the 500–600 nm region, this region is often filtered out to improve

contrast (O'Neil et al., 1983). Overall, however, oil has no specific characteristics that distinguish it from the background (Brown et al., 1996; Taylor, 1992). Therefore, techniques that separate specific spectral regions do not increase detection capability. Some researchers noted that while the oil spectra are flat, that the presence of oil may slightly alter water spectra.

Scanners were used in the past as sensors in the visible region of the spectrum. A rotating mirror or prism swept the field-of-view and directed the light towards a detector. Before the advent of CCD (charge-coupled device) detectors, this sensor provided much more sensitivity and selectivity than video cameras. Another advantage of scanners was that signals were easily digitized and

processed before display. Newer technology has evolved and similar digitization can be achieved without scanning by using a CCD imager and continually recording all elements, each of which is directed to a different field-of-view on the ground. This type of sensor, known as a push-broom scanner, has many advantages over the older scanning types. It can overcome several types of aberrations and errors, the units are more reliable than mechanical ones, and all data are collected simultaneously for a given line perpendicular to the direction of the aircraft's flight. Several types of scanners were developed. Such scanning devices were developed in several countries and technology evaluated (Wang et al., 2010a,b).

It has been known for some time that oil on the water surface is better viewed with polarized lenses. Several workers have noted the polarizing effects of oil on water and have proposed methods to use this phenomenon to distinguish oil (Shen et al., 2011; Yuan et al., 2011).

Sun glitter is a particular problem in visible remote sensing. Sun glitter can sometimes be confused for oil sheens. Several workers have found ways to reduce or to deal with sun glitter (Myasoedov et al., 2012; Zhan et al., 2010).

Video cameras are often used in conjunction with filters to improve the contrast in a manner similar to that noted for still cameras. This technique has had limited success for oil spill remote sensing because of poor contrast and lack of positive discrimination. With new light-enhancement technology, video cameras can be operated even in darkness. Tests of a generation III night vision camera showed that this technology is capable of providing imagery in dark night conditions (Brown et al., 2005a,b).

Hyperspectral imaging is a growing area in remote sensing in which an imaging spectrometer collects hundreds of images at different wavelengths for the same spatial area (Gonzalez et al., 2013). Hyperspectral images are extremely complex, and require advanced processing algorithms to satisfy near real-time requirements in applications such as, mapping of oil spills and chemical contamination. One of the most widely used techniques for analyzing hyperspectral images is spectral un-mixing, which allows for sub-pixel data characterization. This is particularly important since the available spatial resolution in hyperspectral images is typically several meters, and therefore it is reasonable to assume that several spectrally pure substances (called endmembers in hyperspectral imaging terminology) can be found within each imaged pixel. This type of processing is time-consuming and computer intensive. Multi-spectral and hyperspectral sensing was used extensively during recent large spills (Bostater et al., 2012; Bradford and Sanchez-Reyes, 2011; Corucci et al., 2010; Kokaly et al., 2013; Kroutil et al., 2010; Rand et al., 2011; Svejkovsky et al., 2012).

Data in the visible has been subject to many efforts to use mathematical techniques to help distinguish oil from water (Nie and Zhang, 2012; Sun et al., 2013; Wang et al., 2010a,b; Yuan et al., 2011). At this time no automatic processing algorithms are used in the oil spill industry.

Overall, the visible area remains an active research area as well as a practical means of monitoring oil spills. Fig. 4 shows one of the many visible images from the Deepwater Horizon oil spill.

2.3. Infrared

Oil, which is optically thick, absorbs solar radiation and re-emits a portion of this radiation as thermal energy, primarily in the 8–14 μm region (long-wave). As oil has a higher emissivity of infrared than water, oil will after heating emit infrared radiation. Use of infrared is a case where one is measuring the emissions from the oil (Pinel and Bourlier, 2009). In infrared (IR) images, thick oil appears hot, intermediate thicknesses of oil appear cool and thin oil or sheens are not detected. The thicknesses at which these transitions occur are poorly understood, but evidence indicates
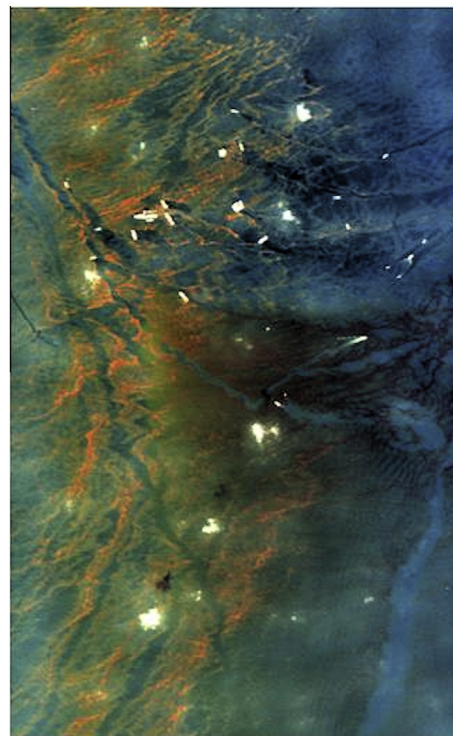

Fig. 4. A visible image of the Deepwater Horizon spill from space (courtesy of NASA). This shows the ease with which photography can be used on large spills with clear weather.

that the transition between the hot and cold layer lies between 50 and 150 μm and the minimum detectable layer is between 10 and 70 μm (Fingas and Brown, 2011). The reason for the appearance of the 'cool' slick may be that a moderately thin layer of oil on the water surface causes destructive interference of the thermal radiation waves emitted by the water, thereby reducing the amount of thermal radiation emitted by the water. This is analogous to the appearance of the rainbow sheen in the visible range. The cool slick would correspond to the thicknesses as observed above, because the minimum destructive thickness would be about 2 times the wavelength which is between 8 and 10 μm. This would yield a destructive interference onset of about 16–20 μm to about 4 wavelengths or about 32–40 μm. The destructive or 'cool' area is usually only seen with test slicks, which is explained by the fact that the more rapidly-spreading oil is of the correct thickness to show this phenomenon. Slicks that have been on the water for a longer period of time usually are thicker or thinner (i.e. sheen) than 16–40 μm. The onset of the hot thermal layer would, in theory, then be at thicknesses greater than this or at about 50 μm. Under circumstances such as high evaporation of a slick, the temperature contrast between water and the oil may not be distinct.

Infrared sensors cannot detect emulsions (water-in-oil emulsions) under most circumstances (Bolus, 1996). This is probably a result of the high thermal conductivity of emulsions as they typically contain 50–70% water and thus do not show temperature differences from the surrounding water.

Most infrared sensing of oil spills takes place in the thermal infrared at wavelengths of 8–14 μm. Specific studies in the thermal infrared show that there is no spectral structure in this region (Salisbury et al., 1993). Tests of a number of infrared systems show that spatial resolution is extremely important when the oil is distributed in windrows and patches. Cameras operating in the 3–5 μm range are only marginally useful (Hover, 1994). Nighttime tests of IR sensors show that there is detection of oil (oil appears cold on a warmer ocean), however the contrast is not as good as

during daytime (Shih and Andrews, 2008a). Further, on many nights no difference is seen. A daytime image of oil using infrared is seen in Fig. 5.

The relative thickness information in the thermal infrared is not useful enough to provide information for oil spill countermeasures. Oil detection in the infrared is not positive, however, as several false targets can interfere, including seaweeds, sediment, organic matter, shoreline, and oceanic fronts. Infrared sensors are reasonably inexpensive, however, and are currently a tool used by the spill remote sensor operator. Infrared cameras are now very common and commercial units are available from several manufacturers.

2.4. Near-infrared

Near infrared (NIR) has not been used much for oil spills in the past. With the advent of NIR bands on the satellites MODIS and MERIS and the airborne AVIRIS, some work has been carried out. Oil spill imaging on all of these sensor platforms was possible during the Deepwater Horizon spill (Bulgarelli and Djavidna, 2012; Etellisi and Deng, 2012). Some researchers have attempted to use the NIR as a means for estimating oil spill thickness (Clark et al., 2010; De Carolis et al., 2012).

2.5. Ultraviolet

Oil shows a high reflectance of sunlight in the ultraviolet range. Ultraviolet sensors can be used to map sheens of oil as oil slicks display high reflectivity of ultraviolet (UV) radiation even at thin layers (<0.1 µm) (Fingas and Brown, 2011). Overlaid ultraviolet and infrared images were used in the past to produce a relative thickness map of oil spills. This technique is largely not used today as the thicknesses are not relevant to oil spill countermeasures. Thicknesses of 0.5–10 mm are needed for countermeasures pur-

poses these are almost 1000 times greater than those indicated by infrared (Brown et al., 1998). Ultraviolet data are also subject to many interferences or false images such as wind slicks, sun glints, and biogenic material (Yin et al., 2010).

2.6. Satellites operating in optical region

The use of optical satellite remote sensing for oil spills has been attempted for many years. In the past there were few satellites with limited passes and thus success was limited by chance to clear days when there was an overpass (Fingas and Brown, 2011). In the past, there were several problems associated with relying on satellites operating in optical ranges, for oil spill remote sensing. The first is the timing and frequency of overpasses and the absolute need for clear skies to perform optical work (Fingas and Brown, 2011). This is particularly true with older satellites with very infrequent overpasses. The chances of the overpass and the clear skies occurring at the same time gave a very low probability of seeing a spill on a satellite image. This point is well illustrated in the case of the Exxon Valdez spill. Although the spill covered vast amounts of ocean for over a month, there was only one clear day that coincided with a satellite overpass, and that was on April 7, 1989 (Fingas and Brown, 2011). Another disadvantage of satellite remote sensing is the difficulty in developing algorithms to highlight the oil slicks and the long time required to do so. For the Exxon Valdez spill, it took more than two months before the first group managed to 'see' the oil slick in the satellite imagery, although its location was precisely known. Fortunately, this has changed with the data availability and better information processing in modern satellites.

New satellites such as QuickBird, WorldView I and II provide more frequent coverage of the earth than the previous satellites. Further the uses of multi-spectral satellites such as MODIS and MERIS have provided new tools for earth observation. Newer findings show that the ability to detect oil in the visible spectrum may be a complex function of conditions, oil types and view angles (Alawadi et al., 2008; Li et al., 2008; Lotliker et al., 2008). The major interference to optical satellite use is the presence of clouds. Another difficulty in dealing with satellite visible imagery is the presence of sun glint, or high reflectivity in certain parts of the image. Sun glint is sometimes severe and can obscure an image and several researchers have made efforts to remove this interference (Grimaldi et al., 2011; Hu, 2011; Liu et al., 2011). There were many uses of visual imagery from satellites during the Deepwater Hori-

Fig. 5. An infrared image of the Gulf spill in 2010. The black objects near the middle and lower portions of the oil are oil. The black objects near the top are islands and shoreline. The oil slick is patchy as the sheen does not show up. This image is from the infrared sensor ASTER on the Terra satellite (NASA).
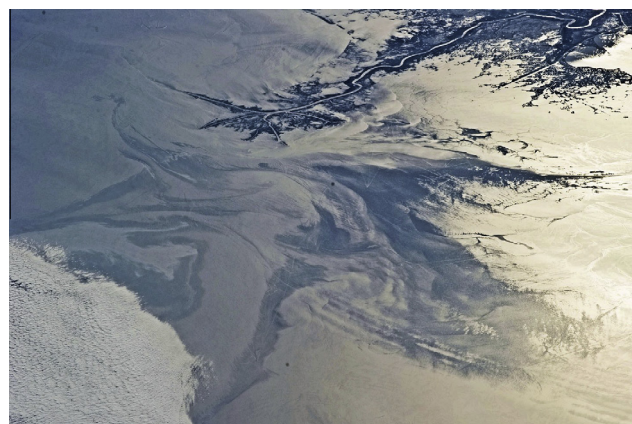
Fig. 6. A view of the Deepwater Horizon spill from an optical satellite. The oil in this case is some of the gray material off the Louisiana coast. Much of the scene is obscured by clouds. This image shows some of the difficulty in discriminating oil using photographic images from space (from USGS).

zon spill in the United States (Leifer et al., 2012). An example of this is shown in Fig. 6.

3. Laser fluorosensors

Laser fluorosensors are sensors that use the phenomenon that aromatic compounds in petroleum oils absorb ultraviolet light and become electronically excited. This excitation is rapidly removed through the process of fluorescence emission, primarily in the visible region of the spectrum (Brown, 2011; Brown and Fingas, 2003a,b; Sarma and Ryder, 2006). Since very few other compounds show this tendency, fluorescence is a strong indication of the presence of oil. Natural fluorescing substances, such as chlorophyll, fluoresce at sufficiently different wavelengths than oil to avoid confusion. As different types of oil yield slightly different fluorescent intensities and spectral signatures, it is possible to differentiate between classes of oil under ideal conditions (see Fig. 7).

Most laser fluorosensors used for oil spill detection employ a laser operating in the ultraviolet region of 308–355 nm (Brown, 2011). There are several commercially-available ultraviolet lasers in the 300–355 nm region including the XeCl excimer laser (308 nm), the nitrogen laser (337 nm), the XeF excimer laser (351 nm), and the frequency-tripled Nd:YAG laser (355 nm). With the excimer wavelength of activation, there exists a broad range of fluorescent response for organic matter, centered at 420 nm. This is referred to as Gelbstoff or yellow matter, which can be easily annulled. Chlorophyll yields a sharp peak at 685 nm. The fluorescent response of crude oil ranges from 400 to 650 nm with peak centers in the 480 nm region.

Most fluorosensors use a technique to open their detectors just at the time when signals return from the surface. This technique is called 'gating'. This vastly increases sensitivity and selectivity. Some fluorosensors are capable of gating their detectors to look below the target surface and some also to look at above the target surface. Work has been conducted on detecting oil in the water column such as occurs with the heavy oil-in-water product, Orimulsion (Brown et al., 2003). This was carried out with a gated fluorosensor which looked at signal returns below the target surface. This work shows that gated laser fluorosensors are capable of detecting oil in the water column as deep as 2 m and easily at 1 m.

The laser fluorosensor is a sampling instrument. The repetition rate of the laser and the ground speed of the aircraft are important in the sampling rate of the surface where the oil contamination is being observed. At ground speeds of 100–140 knots at a laser repetition rate of 100 Hz, a fluorescence spectrum is collected approximately every 60 cm along the flight path. This decreases if the instrument is scanning.

If the sensor were to be gated to look only at signals above the target surface, then it might be useful to look at aerosols such as occur with chemical accidents. Little work has been carried out on this.

Another phenomenon, known as Raman scattering, involves energy transfer between the incident light and the water molecules (Brown, 2011). When the incident ultraviolet light interacts with the water molecules, Raman scattering occurs. This involves an energy transfer between the incident light and water molecules. The water molecules absorb some of the energy as rotational–vibrational energy and emit light at a wavelength which is the difference between the incident radiation and the vibration–rotational energy of the molecule. The Raman signal for water occurs at 344 nm when the incident wavelength is 308 nm (XeCl laser). The water Raman signal is useful for maintaining wavelength calibration of the fluorosensor in operation.

Laser fluorosensors have significant potential as they may be the only means to discriminate between oiled and unoiled seaweeds and to detect oil on different types of shorelines. Tests on shorelines show that this technique has been successful.

Laser fluorosensors have shown high utility in practice and are now becoming essential sensors in many remote sensing packages (Tebeau et al., 2007). The information in the output is unique and the technique provides a unique method of oil identification. The method is analogous to performing chemistry in flight. The typical fluorosensor can provide an abundance of information to the user.

4. Microwave sensors

Microwave sensors are becoming the most commonly used sensors for oil spill remote sensing, particularly the active sensors such as radars.

4.1. Passive microwave sensors

Passive microwave radiometers detect the presence of an oil film on water by measuring the reflection of the surface as excited by the radiation from space. The apparent emissivity factor of water is 0.4 compared to 0.8 for oil (Ulaby et al., 1989). A passive microwave radiometer can detect this emissivity difference and therefore can be used to detect oil. In addition, as the signal changes with thickness, the device can be used to measure thickness. Biogenic materials also interfere and the signal-to-noise ratio is low. In addition, it is difficult to achieve high spatial resolution. One needs resolution in metres rather than the typical tens of metres for a radiometer.

In the past there were extensive efforts in this area (Fingas and Brown, 2011). Many systems have been flown in the past with generally positive results. Focus has generally been on using multiple frequencies to measure thickness. This will be discussed in greater detail later in this paper. Several workers have focussed on using passive microwave to image oil slicks as a remote sensing tool (Yujiri et al., 2003; Calla et al., 2011, 2013).

4.2. Radar

Capillary waves on the ocean reflect radar energy, producing a 'bright' image known as sea clutter. Since oil on the sea surface dampens capillary waves, the presence of an oil slick might be detected as a 'dark' sea or one with an absence of this sea clutter
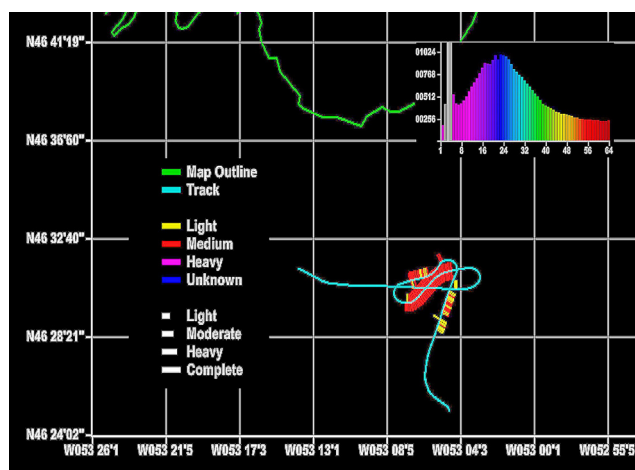
Fig. 7. Portions of a real-time fluorosensor output display. The oil detections are shown as bars along the mapped flight path. The color of the bars shows the type of oil measured. The length of the bar shows the aerial coverage. At each point along the flight path the spectrum of the target is also displayed. (From Environment Canada.)

(Nunziata et al., 2008; Li et al., 2011). Oil slicks are not the only phenomena that are detected in this way. There are many interferences or false targets, including fresh water slicks, wind slicks (calm areas), wave shadows behind land or structures, shallow seaweed beds that calm the water just above them, glacial flour, biogenic oils, and whale and fish sperm (Gens, 2008). As a result, radar can be problematic in locations where fresh water inflows, ice, and other features produce hundreds of such false targets. Liu et al. (2010) showed that even with extensive processing, that false hits on SAR imagery were 20%, that is 20% of the images reported as oil, were still look-alikes. Despite these limitations, radar is an important tool for oil spill remote sensing because it is the only sensor that can be used for searches of large areas and it is one of the few sensors that can detect anomalies at night and through clouds or fog.

Side-looking radar has completely different geometries than the more-familiar search radars. Search radar systems, such as those frequently used by the military, cannot be used for oil spills as they usually remove the clutter signal, which is the primary signal of interest for oil spill detection. Furthermore, the signal processing of this type of radar is optimized to pinpoint small, hard objects, such as periscopes. This signal processing is very detrimental to oil spill detection.

The two basic types of imaging radar that can be used to detect oil spills and for environmental remote sensing in general are Synthetic Aperture Radar (SAR) and Side-Looking Airborne Radar (SLAR). The latter is an older, but less expensive technology, which uses a long antenna to achieve spatial resolution. Synthetic aperture radar uses the forward motion of the aircraft to synthesize a long antenna, thereby achieving good spatial resolution, which is independent of range, with the disadvantage of requiring sophisticated electronic processing. While more expensive, the SAR has greater range and resolution than the SLAR. Comparative tests show that SAR is vastly superior (Mastin et al., 1994). SLAR has predominated airborne oil spill remote sensing, primarily because of the lower price.

Experimental work on oil spills has shown that X-band radar yields better data than L- or C-band radar (Kim et al., 2010; Minchew et al., 2012; Yang et al., 2009). The availability of extensive oil for a long period of time on the Deepwater Horizon spill allowed several parties to study various aspects of radar including band relationships (Minchew et al., 2012). In summary, X band has advantages over other bands, however C band radar can yield good oil spill imagery and L-band radar provides useable imagery of oil spills.

Several different polarizations exist based on vertical (V) and horizontal (H) electromagnetic wave propagation. Typically transmission and reception are in the same polarization, i.e. VV or HH (transmission polarity then reception polarization). But, there are actually 4 poles available: HH, VV, HV and VH. Use of all four of these is designated as quadrapole. It has also been shown that vertical antenna polarizations for both transmission and reception (VV) yield better results than other configurations, especially for airborne radar, however at the angles used for satellite, the polarizations are less significant in terms of image discrimination (Nunziata et al., 2012, 2013; Solberg, 2012). Some workers noted that VV polarization tends to be more suitable for oil pollution detection when winds are strong and HH when winds are light although this was observational (Kuzmanic and Vujovic, 2010). However, the dependency of HH polarization on the incidence angle is greater than that of VV polarization. This means that if the incidence angle is small, the difference in intensity between HH and VV polarization is small, but if the incidence angle is large, the VV image on the sea is brighter than the HH image. This suggests that generally the VV image is better for detecting oil spills (Solberg, 2012).

Several workers have noted that polarimetric SAR can provide powerful discrimination between slicks and look-alikes (Hensley et al., 2012; Salberg et al., 2012; Skrunes et al., 2012). Additionally, phase differences can be used to detect oil and perhaps to discriminate these from other phenomena (Migliaccio et al., 2009, 2011). Further work on polarimetric SAR continues and this shows promise for future work.

The ability of radar to detect oil is limited by sea state. Sea states that are too low will not produce enough sea clutter in the surrounding sea to contrast with the oil and very high seas will scatter radar sufficiently to block detection inside the wave troughs. Indications are that minimum wind speeds of 1.5 m/s (~3 knots) are required to allow detectability and a maximum wind speed of 6–10 m/s will again remove the effect (Hühnerfuss et al., 1996; Akar et al., 2011). The most accepted limits are 1.5 m/s (~3 knots) to 10 m/s (~20 knots). This limits the environmental window of application of radar for detecting oil slicks.

Radar is also subject to interferences that appear to be like oil, i.e. substances or phenomena that dampen waves. These look-alikes include: low wind areas, areas sheltered by land, rain cells, organic films, grease ice, wind fronts, up-welling zones, oceanic fronts, algae blooms, current shear zones, etc. Extensive effort has been placed upon removing these look-alikes from imagery and automating the process of slick detection (Anderson et al., 2010; Ferraro et al., 2010; Muellenhoff et al., 2008; Shi et al., 2008; Shu et al., 2010; Sipelgas and Uiboupin, 2007; Topouzelis et al., 2008, 2009a). This issue is relevant to both satellite and airborne SAR systems.

In summary, radar optimized for oil spills is useful in oil spill remote sensing, particularly for searches of large areas and for nighttime or foul weather work. The technique is highly prone to false targets, however, and is limited to a narrow range of wind speeds (1.5–10 m/s). Because of the all-weather and day-night capability, radar is now the most common means of oil spill remote sensing in offshore areas. Fig. 8 shows successful application of radar to an offshore spill.

4.3. Satellite radar systems

Currently many different radar systems exist, giving scientists a choice of configurations, bands and polarizations. Some of these studies and systems will be described here. Table 1 lists some of the current and proposed satellites for radar satellites. Most radar
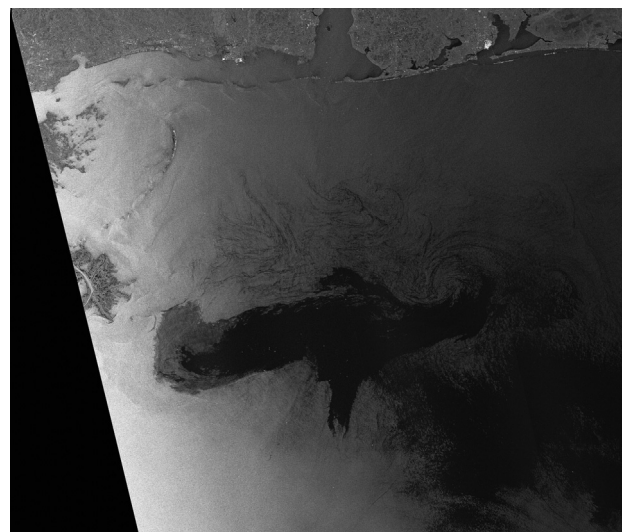

Fig. 8. The Deepwater Horizon as imaged by Radarsat (EOSANP).

Table 1
Current and future satellite-borne SAR sensors.

Satellite	Launch date	Owner/operator	Band
RADARSAT-2	2007	Canadian Space Agency	C
TerraSAR-X	2007	German Aerospace Centre	X
Tandem -X	2010	German Aerospace Centre	X
Cosmos Skymed-1/2	2007, 2010	Italian Space Agency	X
TecSAR	2008	Israel Aerospace Industries	X
Kompsat-5	2013	Korean Space Agency	X
Sentinel-1	2013	European Space Agency	C
RADARSAT-Constellation (3-satellites)	2018	Canadian Space Agency	C

satellites have a variety of coverages, a variety of resolutions and polarizations. As most radar satellites are designed for a lifetime of 5 years, the suite of satellites available is constantly changing. Some satellites have lasted for 17 years and others for only one year.

4.4. Radar image processing

Radar detection of oil spills is highly susceptible to false images or look-alikes, thus much work has taken place on means to differentiate oil slicks and false targets as well as methods to automate the analysis process (Topouzelis et al., 2009b). The discussion in this subjection is relevant to both satellite and airborne SAR systems.

The following discussion is organized by the generic form of processing:

4.4.1. Quality assessment
The first step in most radar image analysis is to assess the quality of the image, to find out if it will be useful and what particular properties it has (Ferraro et al., 2012; Vespe and Greidanus, 2012). The image may not have sufficient quality to proceed.

4.4.2. Speckle removal
Radar is subject to receiving strong reflections from objects or surfaces that are directly aligned to an antenna. This is a problem in imagery as the 'bright' spots are too high in amplitude to allow for further processing. Therefore, several algorithms for removal of speckle have been developed (Liu et al., 2013). Since speckle is temporary, multi-look imaging is one way to decrease speckle by a large amount (Migliaccio et al., 2007; Migliaccio, 2005).

4.4.3. Noise removal
All radar images contain some noise. This noise may be large enough to interfere with subsequent analysis. In this case the noise is removed (Liu and Wang, 2012).

4.4.4. Wind field elimination
Low or high wind areas do not show oil spills. Therefore, it is useful if these areas can be flagged in an image to improve interpretation (Mera et al., 2012; Muellenhoff et al., 2008). One traditional method of doing this is to do a separate wind file at the same scale as the radar image and overlay this on the radar image. Some researchers have flagged areas inside radar images where oil would not be noted because of low or high wind conditions.

4.4.5. GIS to remove known shoreline and other effects
As land and shoreline is basically an interference to oil detection on water, it is useful to have these flagged on radar images. This can be done with Graphical Information Systems (GIS) which can flag off areas close to land on radar images (Assilzadeh and Gao, 2008). This is particularly useful for automatic oil detection. Individuals looking at images typically will find the land and shore-

line. Another useful function of GIS-processed images is to flag out areas where there are weed beds or known algae infestations.

4.4.6. Edge detection
One method that has led to some automation is the edge detection of oil spills in radar imagery (Zhang et al., 2010, 2012). Edge detection is the use of mathematical algorithms to delineate the edges between water and oil. This is often a preliminary step to further analysis. In other cases it is an end product where the slicks (or potential slicks) are all circled.

4.4.7. Texture analysis
Texture analysis is sometimes used to detect what is oil or not on radar imagery (Tello et al., 2007; Zhang et al., 2008). What is done is to look at the surface characteristics. Oil has a uniform texture. Sea has a less uniform texture. Look-alikes may sometimes be separated on this basis, but other times not.

4.4.8. Shape analysis
Some researchers claim that oil has unique shapes over look-alikes and this has been used to discriminate slicks (Chaudhuri et al., 2012; Mishra et al., 2011).

4.4.9. Fuzzy logic
Fuzzy logic is a branch of mathematics that uses non-linear techniques to predict outcomes. Known outcomes with certain inputs are used to program a model to predict which of the dark areas on a slick are oil and which are not. Many researchers have used this type of model to discriminate oil in radar images (Garcia-Pineda et al., 2008; Morales et al., 2008; Robson et al., 2006).

4.4.10. Neural networks
This is another branch of mathematics that uses a programmed set of data to predict outcomes. Known outcomes with certain inputs are used to program a model to predict which of the dark areas on a slick are oil and which are not. This relies on human interpretation of known slick images to program the neural network model. Neural networks are models that are 'trained' on standard inputs and outputs and then tested on inputs with or without known outputs. Many workers have developed neural network models to screen radar images (Ozkan et al., 2011; Singha et al., 2012, 2013; Topouzelis et al., 2007, 2008, 2009b).

4.4.11. Others
There are many other approaches to modeling the determination of oil slicks in radar images. Some of these are classified as 'filters', which use specific algorithms to analyze images.

A similar approach is to use a classification scheme that incorporates some of the features of several approaches above (Akar et al., 2011; Engdahl et al., 2012; Hu et al., 2012; Marghany and Hashim, 2011; Topouzelis and Psyllos, 2012).

4.4.12. Automatic systems

Several 'automatic' systems have been designed for slick detection in the past (Solberg and Theophilopoulos, 1997). In recent years automatic systems have given way to systems involving smart algorithms and manipulated by operators (Martinis et al., 2012; Tian et al., 2008; Vespe et al., 2011).

4.5. Ship-borne radar oil spill detection

Ship-borne radar has similar limitations to airborne and satellite-borne radar and the additional handicap of low altitude, which restricts its range to between 8 and 30 km, depending on the height of the antenna (Gangeskar, 2004). Ordinary ship radars can be adjusted to reduce the effect of sea clutter de-enhancement, however specialized units perform much better for oil slick detection (Nøst and Egset, 2006; Suo et al., 2012). Ship-borne radar successfully detected many slicks and at least eight commercial systems are now available.

5. Slick thickness measurements

Slick thickness measurements are now at an early infancy of development (Fingas, 2012). There are many proposed solutions. There are numerous problems in the field. First and foremost, there are few available field measurement techniques. Thus we know little about how slicks are distributed and what the ranges of thickness might be. Further we don't really understand how this relates to oil type, sea conditions, etc. Water-in-oil emulsions form and these have quite different appearances from non-emulsified slicks. The few thickness values that exist may be incorrect. There are several techniques that measure slick thickness around 0.1–10 μm (0.0001–0.001 mm), but these are not useful to oil spill work. One thing that must be borne in mind is that useful thickness measurements need to be between 0.0.5 and 10 mm to be useful for oil spill countermeasures (Brown et al., 1998).

5.1. Passive microwave

Passive microwave uses ambient microwave radiation from space to measure oil thickness (Skou et al., 1983; Pelyushenko, 1993). The microwave signal itself is reflected within the oil layer creating a resonance that can be detected. As the signal is cyclical with respect oil thickness, more than one frequency must be measured to measure oil thickness. The systems require calibration, usually carried out by sensing plastic sheets of the appropriate thickness. Currently passive microwave instruments are the only ones being used for oil thickness measurements. Fig. 9 shows the output from a processed set of images of a slick.

5.2. Acoustic travel time

This technology uses a laser to generate a pulse in the oil layer from an aircraft (Brown and Fingas, 2003a,b; Brown et al., 2005a,b). Then the travel of the acoustic pulse through the oil is measured by another laser. The signal is decoded to yield travel time and thus oil thickness. The sensing process is initiated with a thermal pulse created in the oil layer by the absorption of a powerful CO_2 laser pulse. Rapid thermal expansion of the oil occurs near the surface where the laser beam was absorbed, which causes an acoustic pulse of high frequency. The acoustic pulse travels down through the oil until it reaches the oil-water interface where it is partially transmitted and partially reflected back towards the oil-air interface, where it displaces the oil's surface. The time required for the acoustic pulse to travel through the oil and back to the surface again is a function of the thickness. The displacement of the surface
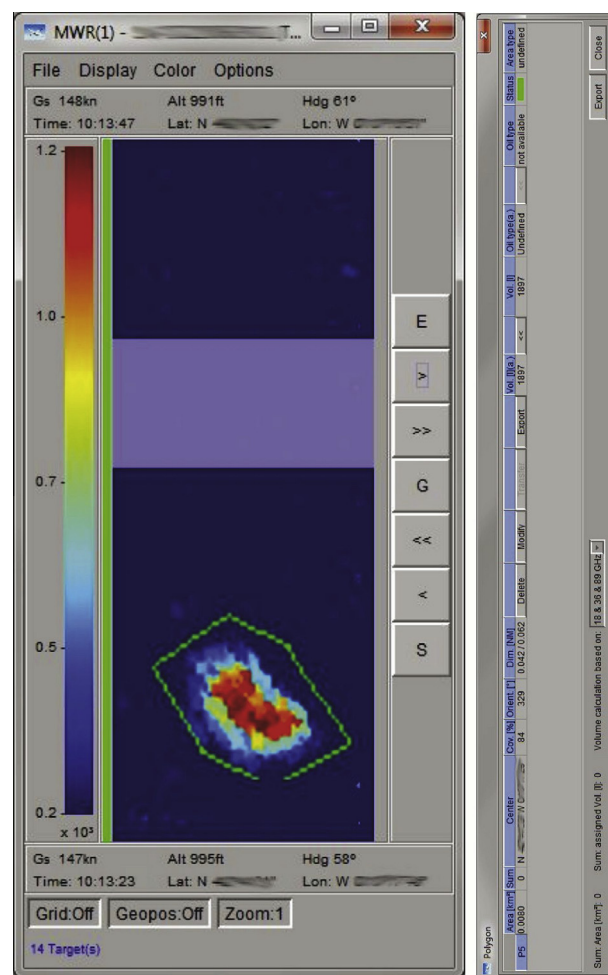

Fig. 9. An image of a slick characterized by microwave (Communication from Nils Robbe, Optimare, 2013). The colors of the image represent thicknesses and the scale is on the left hand side of the image display (ranges from 0.2 to 1.2 mm in this case). This is an image from the usual aircraft display and several pieces of information are normally available including location, area of slick (here this is 0.008 km², yielding a volume of 1897 L). The data were measured using a 3-band passive microwave imager operating at 18, 36 and 89 GHz.

is measured by a second laser probe beam (Nd:YAG) aimed at the surface. Motion of the surface induces a phase or frequency shift (Doppler shift) in the reflected probe beam. This phase or frequency modulation of the probe beam can then be demodulated with an interferometer. The resulting signal then gives the oil thickness. A prototype instrument has been successfully tested to date.

5.3. Visual

Historically it was thought that thickness could be simply color-coded to its appearance on water (Fingas, 2012). While this is partially true for thin slicks, after about 8 μm, this is no longer the case. In fact, reliably only sheen (0.1 μm to about 1 μm), rainbow sheen (about 1–3 μm) and thicker oil (>3 μm) can be gauged by appearance and color. The sheen is caused by the reflectance of oil. The rainbow sheen is caused by multiple internal reflections of light in the oil and the fact that at these thicknesses oil is partially transparent. Thicker oil than rainbow sheen becomes optically thick and absorbs much of the light (Fingas, 2012; Cong et al., 2012).

Many different codes were developed – largely based on older work. The findings of the research to date include the following:

1. The utility of thicknesses derived from oil color codes is limited. The only reliable color codes are the very thin ones (Fingas, 2012; Brown et al., 1998). Most of the oil is located in the thick portions of the slick. For larger spills the appearance codes are not useful.
2. The only reliable thickness indications are the thin sheen and the rainbow portions. The rainbow portion is the only unique thickness range at about 0.2–about 3 μm (Fingas, 2012). This is illustrated in Fig. 10.
3. There are many influences on appearance including sun angle with respect to viewer; view angle; oil type; sea conditions; water coloration; presence of debris; etc. (Fingas, 2012).
4. There is no supporting evidence for any color differences or relationships for the thicker portions of the slick (Fingas, 2012; Brown et al., 1998).

5.4. Near-IR absorption

A proposal by a group of scientists is that spectroscopic analysis of adsorption in the near infrared (NIR) reveal chemical details of hydrocarbons (Clark et al., 2010; Leifer et al., 2011). They propose that this can be related to oil thickness. Near infrared data are collected using high resolution devices. The reflectance data is then subjected to spectroscopic analysis and related to a calibration table. A method to analyze absorptions due to specific materials is called absorption-band depth mapping. This then is purported to yield slick thickness. Some work was carried out on the Deepwater Horizon spill. No further information on this proposed method has been published.

5.5. Infrared

As the infrared appears to show a higher thickness gradation, several parties have suggested that infrared brightness could be used as a thickness scale. Over the years there have been many attempts to 'calibrate' various systems to measure oil thickness, all to no avail. Surface temperatures should not be confused with internal temperatures. IR exclusively measures surface temperatures. Some researchers have carried out a series of laboratory and tank tests to determine if there was a correlation between infrared brightness and slick thickness (Brown et al., 1998; Shih and Andrews, 2008b). There was no correlation, indicating that the brightness of the infrared image does not vary with slick thickness. It was found that the infrared emission of the slick is constant after a certain minimum thickness is reached.

5.6. Laser trigonometry

Some workers have tried to use the assumption that the oil layer is transparent, therefore the differences in reflection from the water surface and the top of the oil layer could yield a thickness measurement (Lu et al., 2012). But since oil is not transparent, these methods are, in actuality, not promising technologies.

5.7. Radar polarimetry

Kasilingam (1995) proposed that polarimetric radar might be used to measure spill thickness. Polarimetric radar uses both quadrants of propagation and return to characterize a target (e.g. HH, VV, HV, VH). Since there was no algorithm available for this measurement, he suggested that a two-scale resonant model be used to derive a measurement algorithm. The scattering coefficients were found to be a function of the thickness of oil slicks and the oil dielectric constant. The scattering coefficients were converted to Stokes matrices. These data are in turn used to train a neural network to find the optimal polarization and to extract slick thickness. The accuracy of these measurements was calculated. The conclusion was that a 33 GHz SAR would be optimal for conducting such measurements. This theory was never tested in practice.

5.8. Sorbents or oil recovery

The use of sorbents has been suggested and practiced by many (MacDonald et al., 1993). The practice is to apply a sorbent in the field and then take the oil-soaked sorbent home and analyze the amount of oil in it. There are several problems with using sorbents. These include: presumption that the sorbent picks up only that oil it overlays and not more; that the sorbent picks up all the oil over which it lays; and that the oil in the sorbent can be accurately quantified. Furthermore, the disturbance of taking the measurement is significant and if taken from a boat, the approach of the boat changes the thickness in the area. A study of the laboratory use of sorbents to measure slick thickness showed that there were many problems and that the variance of sorbent analysis was about 40% in a laboratory setting (Goodman and Fingas, 1988). It was estimated that the field variance was as much as 10 times this value, rendering this technique entirely useless. Another technique used by was to place an acrylic sheet directly into the slick and then pull it out (Svejkovsky and Muskat, 2006). The oil was scrapped off and measured by volume. The assumption was that the oil on the side of the plate was constantly being adsorbed. This method is very doubtful as to its actual relation to slick thickness.

5.9. Spreading rates and wave containment

Goodman et al. (2004) set up a series of small test tanks to measure the spreading of oil in an attempt to determine if there was such a thing as an average thickness. The tanks were rapidly filled with oil and monitored with a camera to measure the spreading rate. This test showed that for this oil type (a Mexican crude) that spreading was differential and there was no average thickness. Boniewicz-Szmyt et al. (2007) carried out some laboratory experi-
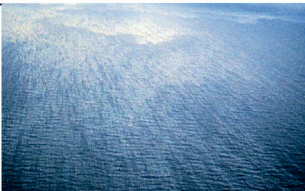
Approximate Slick Thickness (μm)	Oil Appearance	Photographic Example
0.05 to 0.2	Silvery Sheen	
0.3 to 3	Rainbow Sheen	
>3	Oil Colored Brown to Black	

Fig. 10. The appearance of thin films of oil on water. The black and brown areas show the range of colors in this thickness regime. This is the maximum that can be stated about oil thickness definitively. (For interpretation of the references to color in this figure legend, the reader is referred to the web version of this article.)

ments using optical methods to measure spreading rates. They calculated spreading rates and equilibrium thicknesses of 0.02–1.25 cm. These thicknesses are obviously far too great for typical crude and fuel oils. Other attempts to calculate equilibrium thicknesses have not been successful in actual practice (Fay, 1969). It is suggested that final thicknesses are a function of many factors including oil properties, wind, sea conditions, temperature, etc.

Others have looked at the effect of waves, hoping that the containment in the bottom of waves might provide an answer (Kordyban, 1982). Waves were studied and it was found that waves do not part the oil, but simply thin them at the top. Thus, this aspect cannot be used to measure oil amounts.

5.10. Spectroscopic differences

Several parties have noted the differences in oil reflectivity or absorbency at difference wavelengths and different thicknesses (Lu et al., 2012; Shih and Andrews, 2008b). The techniques varied. Some found that the minimum thickness of various oil types varied and thus might be used for detection (Wettle et al., 2010). Others used laboratory measurements of red and infrared reflectance to scale satellite observational data (Byfield and Boxall, 1999). Others used reflectivity in the visible (De Beaucoudrey et al., 2003; Morinaga et al., 2003; Xiao and Tian, 2012). Others related various aspects in multi-spectral imagery to slick thickness (Lennon et al., 2006; Li et al., 2012). Several workers 'calibrated' spectral regions by controlled experiments in the laboratory or the field (Cong et al., 2012; Lu et al., 2013; Svejkovsky et al., 2008; Zhan et al., 2010). The physics behind these proposed methods is lacking in most cases. To date there have been no absolute confirmations that any of these methods yields reliable oil spill thickness values.

5.11. Radar surface damping

As oil on the sea is detected by the damping of capillary waves at wind speeds of about 3–8 m/s, some researchers felt that this might be progressive with spill thickness. Some have tried to correlate the area of dampened slicks with the wind speed and thickness (Hühnerfuss et al., 1989; Jones, 2001; True et al., 1994). Success was not reported.

5.12. Light polarization differences between oil and water

Some researchers suggest that light is polarized between oil and water. Thus measuring the difference in reflected light polarization between oil-covered sea and water, one could supposedly measure thickness (Sun et al., 2011). This has not been proven.

5.13. Laser fluorescence

Some workers proposed that the fluorescent return was different at different thicknesses and at different wave lengths (Viser, 1979). This would then yield thickness measurements. This has never been proven.

5.14. Water Raman suppression

It is relatively well-known that laser fluorosensors activate what is known as water Raman signals. Oil slicks rapidly dampen this signal by absorption, beginning at very small thicknesses (probably less than 1 μm). Some workers have tried to calibrate these signals. These thicknesses are too low to be of consequence to oil spills. The Raman signal for water occurs at 344 nm when the incident wavelength is 308 nm (XeCl laser) (Fingas and Brown, 2011). The water Raman signal is useful for maintaining wavelength calibration of the fluorosensor in operation. The point

at which the Raman signal is entirely suppressed depends on the type of oil, since each oil has a different absorption coefficient (Hoge and Swift, 1980; Piskozub et al., 1997). The Raman signal suppression has led to estimates of sensors detection limits of about 0.05–0.1 μm (Lennon et al., 2006; Brown et al., 2005a,b; Patsayeva et al., 2000). It should be re-emphasized that this thickness is well below that of interest for oil spill countermeasures.

5.15. Electrical conductivity

The presence of an oil film along with water between two electrodes could, in theory, be detected by electrical measurement (Denkilkian et al., 2009; Koulakezian et al., 2008). This method could then be implemented in buoys which could transmit the signal back to a central location.

5.16. Laser interferometry

There is a proposal that laser holography might be used to measure oil spill thickness. This would require oil to be at least semi-transparent in the thickness being measured. This method works by the fact that different thickness layers cause different diffraction patterns (Kukhtarev et al., 2011). Reading these different diffraction patterns may result in a measurement of the thickness of oil. Although tested in the laboratory it has not been shown to be viable at thicknesses of concern nor in the field.

5.17. Ultrasound

As oil/water and air/water interfaces reflect acoustic pulses, thicker layers of oil can be measured using ultrasonic measuring devices (Sumimoto et al., 1986; Brown et al., 1998). This has been carried out from the sub-surface and the surface. The method is only applicable for thicker slicks and during quiescent conditions. This has been applied in the laboratory and in test tanks.

5.18. Thermal conduction time

Rapid heating of a thin oil layer produces thermal profiles which are related to oil thickness (Reimer and Rossiter, 1987). In this technique, known as 'thermal mapping', a laser is used to heat a region of oil and the resultant temperature profiles created over a small region near this heating are examined using an infrared camera. Extensive work would be needed to yield actual thickness measurements.

6. Detection of oil in the water column and on the sea bottom

Many different techniques have been tried for underwater oil detection (Michel, 2011). First, the division should be made between oil in the water column or floating on a pycnocline, and oil on the bottom. Quite different physics and conditions can apply to these different situations. The most common situation is that of oil on the bottom of the particular water body.

6.1. Ultrasonics

Ultrasonics has been used, with some degree of success, to detect oil on the bottom and in the water column (Eriksen, 2013; Medialdea et al., 2008; Weber et al., 2012; Wendelboe et al., 2009). In the water column, oil droplets scatter acoustic signals which are then detected. On a water body floor that contains harder material such as consolidated mud or rock, oil will appear as a softer, absorbing material. The acoustic properties of sunken oil

are sometimes different from the other bottom materials, leading to acoustic detection.

6.2. Laser fluorosensors

Laser fluorosensors use ultraviolet lasers to fluoresce aromatic compounds in oils. The light is collected by the fluorosensor using a telescope and a sensitive detector. The resulting data results in a spectrum which is unique to oil. The detection of oil in the water column is limited to about a 2 m depth in clear water with a wavelength of 3085 nm because of the attenuation of the laser signal in the water column. The fluorosensor for underwater detection use a technique to open their detectors just at the time when signals return from the selected target. This technique is called 'gating'. Some fluorosensors are capable of gating their detectors to look below the target surface. Work has been conducted on detecting oil in the water column such as occurs with the heavy oil-in-water product, Orimulsion (Brown et al., 2003). This was carried out with a gated fluorosensor which looked at signal returns below the target surface. This work shows that gated laser fluorosensors (operating at 308 nm) are capable of detecting oil in the water column as deep as 2 m and easily at 1 m in clear water. Penetration in turbid water would be limited to a lesser depth.

6.3. Cameras

Cameras for underwater application are common as are sources of illumination for such cameras. In cases where the oil shows up differently than the bottom material, detection and mapping are simple. Oil in the water column is not readily seen by cameras, unless it is in high concentrations. Oil on the bottom has successfully been mapped by underwater cameras, often mounted on sleds (Michel, 2011; Pfeifer et al., 2008). The problems with this technique are the bottom visibility - often insufficient to discriminate, and the difficulty in towing the camera vehicle as slow as 1 knot, the necessary speed.

6.4. Chemical analysis

Oil in the water column can be detected by a number of chemical means such as taking a sample and taking it to the surface for further analysis, in-situ fluorometry and in-situ mass spectrometry. Recently, in-water techniques have evolved and sophisticated instrumentation is also available in underwater housings to provide direct results to surface vessels (Camilli et al., 2009).

7. Detection of oil with and under ice or snow

The difficulties in detecting oil in or under ice or snow are numerous (Fingas and Brown, 2013). Ice is always a heterogeneous material and incorporates air, sediment, salt, and water, any of which may present false oil-in-ice signals to the detection mechanisms. In addition, snow on top of the ice or even incorporated into the ice adds complications. During freeze-up and thaw in the spring, there may not be distinct layers of water and ice. There are many different types of ice and different ice crystalline orientations. Snow is also somewhat heterogeneous and may consist of several layers with different densities. Furthermore oil may penetrate snow easily and thus move to the sub-surface of the snow, which may be ice or soil.

There are few off-the-shelf solutions to these problems (Fingas and Brown, 2013). Currently most technologies are either under development or are still being considered. Many acoustic techniques were tried and it was found that acoustic detection of oil was possible because oil behaves as a solid in acoustic terms and

transmits a shear wave. Furthermore, there is an angular dependence to these phenomena and it can be used to distinguish between the many interferences in ice such as air bubbles, and oil. This technology has not however, been pursued or commercialized.

Radio frequency methods such as ground penetrating radar have been tried for both oil under ice and oil under snow (Bradford et al., 2010). The method may not provide sufficient discrimination for positive oil detection in actual spills.

Several other oil-in-ice detection schemes have been assessed and tried including, nuclear magnetic resonance, gamma ray detection, standard acoustic thickness probes, fluorosensor techniques, and augmented infrared detection (Fingas and Brown, 2013). Each of these showed potential in theory and some during tank tests. Further development and testing on these proposed methods are required.

The technology for detecting surface oil with ice is further advanced. Laser fluorosensors show the greatest potential for detection of oil when the oil is exposed to the surface (Fingas and Brown, 2013). There is very limited potential for optical techniques, particularly for infrared techniques. Radar and microwave do not show potential for this application.

8. Concluding remarks

The last decade has seen great strides in some areas and little progress in others. It should be noted that oil spills are seen by sensor manufacturers as a niche market and little development effort specifically for oil spills, has occurred. For offshore oil spills, the use of satellite radar has expanded very rapidly. The availability of data from several satellites has greatly increased the utility of this technique. Despite the limitations of winds and presence of look-alikes, the technique of satellite radar has predominated the detection and mapping of offshore spills. This trend is likely to continue and expand for some time to come. The application of other techniques to offshore oil spills has lagged far behind.

There is little development for near-shore and land spills compared to that for offshore spills. The technology is still similar to that of a decade ago. A similar situation exists for sub-surface spills and for oil in ice situations.

Two specific sensors that show potential are the passive microwave radiometer for measuring thickness at sea, and the laser fluorosensor for a variety of sensing applications. Both sensors require some more development and extensive commercialization.

References

Akar, S., Suezen, M.L., Kaymakci, N., 2011. Detection and object-based classification of offshore oil slicks using ENVISAT-ASAR images. Environ. Monit. Assess. 183 (01-April), 409–423.

Alawadi, F., Amos, C., Byfield, V., Petrov, P., 2008. The application of hyperspectral image techniques on modis data for the detection of oil spills in the RSA. SPIE, 71100Q.

Anderson, S., Raudsepp, U., Uiboupin, R., 2010. Oil spill statistics from SAR Images in the North Eastern Baltic Sea Ship Route in 2007–2009. IGARSS, 1883.

Andreou, C., Karathanassi, V., 2011. Endmember detection in marine environment with oil spill event. Proc. SPIE – Int. Soc. Opt. Eng. (8180), 81800P.

Assilzadeh, H., Gao, Y., 2008. Oil spill emergency response mapping for coastal area using SAR imagery and GIS. Proc. Oceans Mar. Technol. Soc., 5151820.

Bolus, R.L., 1996. Airborne testing of a suite of remote sensors for oil spill detecting on water. In: Proceedings of the Second Thematic International Airborne Remote Sensing Conference and Exhibition, ERIM, III, pp. 743–748 .

Boniewicz-Szmyt, K., Pogorzelski, S., Mazurek, A., 2007. Hydrocarbons on sea water: steady-state spreading signatures determined by an optical method. Oceanologia 49 (3), 413–437.

Bostater Jr., C.R., Frystacky, H., Levaux, F., 2012. Enhanced Data fusion protocol for surface and subsurface imaging of released oil in littoral zones. In: Proceedings of the International Offshore and Polar Engineering Conference, pp. 808–814.

Bradford, B.N., Sanchez-Reyes, P.J., 2011. Automated oil spill detection with multispectral imagery. Proc. SPIE – Int. Soc. Opt. Eng. 8030, 80300L.

Bradford, J.H., Dickins, D.F., Brandvik, P.J., 2010. Assessing the potential to detect oil spills in and under snow using airborne ground-penetrating radar. Geophysics 75 (2), G1–G12, GPYSA70000750000020000G1000001.

Brown, C.E., 2011. Laser fluorosensors. Oil Spill Sci. Technol., 171–184.

Brown, C.E., Fingas, M.F., 2003a. Review of the development of laser fluorosensors for oil spill application. Mar. Pollut. Bull. 477, 485–492.

Brown, C.E., Fingas, M.F., 2003b. Development of airborne oil thickness measurements. Mar. Pollut. Bull. 47 (09–December), 485–492.

Brown, H.M., Bittner, J.P., Goodman, R.H., 1996. The limits of visibility of spilled oil sheens. In: Proceedings of the Second Thematic International Airborne Remote Sensing Conference and Exhibition, Erim Conferences, III, pp. 327–338.

Brown, H.M., Baschuk, J.J., Goodman, R.H., 1998. Infrared sensing and the measurement of oil slick thickness. AMOP (2), 805–810.

Brown, C.E., Marois, R., Gamble, R.L., Fingas, M.F., 2003. Further studies on the remote detection of submerged orimulsion with a range-gated laser fluorosensor. AMOP, 279–286.

Brown, C.E., Fingas, M.F., Monchalin, J.-P., Neron, C., Padioleau, C., 2005a. Airborne oil slick thickness measurements: realization of a dream. In: Proceedings of the Eighth International Conference on Remote Sensing for Marine and Coastal Environments, Altarum.

Brown, C.E., Fingas, M.F., Marois, R., 2005b. Oil spill remote sensing flights in the coastal waters around newfoundland. In: Proceedings of the Eighth International Conference on Remote Sensing for Marine and Coastal Environments, Altarum, 8 p.

Bulgarelli, B., Djavidnia, S., 2012. On MODIS retrieval of the marine environment. IEEE Geosci. Remote Sens. Lett. 9 (3), 398–402 (6069530).

Byfield, V., Boxall, S.R., 1999. Thickness estimates and classification of surface oil using passive sensing at visible and near-infrared wavelengths. IGARSS (3), 1475–1477.

Calla, O.P.N., Ahmadian, N., Hasan, S., 2011. Estimation of Emissivity and Scattering Coefficient of Low Saline Water Contaminated by Diesel in Cj Band (5.3 GHz) and Ku Band (13.4 GHz). Indian Journal of Radio and Space Physics 40 (5), 267–274.

Calla, O.P.N., Dadhich, H.K., Singhal, S., 2013. Oil Spill Detection Using SSM/I Satellite Data Over Bombay High Location in Arabian Sea. Indian Journal of Radio and Space Physics 42 (1), 52–59.

Camilli, R., Bingham, B., Reddy, C.M., Nelson, R.K., Duryea, A.N., 2009. Method for rapid localization of seafloor petroleum contamination using concurrent mass spectrometry and acoustic positioning. Mar. Pollut. Bull. 58 (10), 1505–1513.

Chaudhuri, D., Samal, A., Agrawal, A., Sanjay, A., Mishra, A., Gohri, V., Agarwal, R.C., 2012. A statistical approach for automatic detection of ocean disturbance features from sar images. IEEE J. Select. Topics Appl. Earth Observ. Remote Sens. 5 (4), 1231–1242 (6210409).

Clark, R.N., Swayze, G.A., Leifer, I., Livo, K.E., Lundeem, S., et al., 2010. A method for qualitative mapping of thick oil using imaging spectroscopy. United States Geol. Survey, <http://pubs.usgs.gov/of/2010/1101/>.

Cong, L., Nutter, B., Liang, D., 2012. Estimation of oil thickness and aging from hyperspectral signature. In: Proceedings of the IEEE Southwest Symposium on Image Analysis and Interpretation, 6202491, pp. 213–216.

Corucci, L., Nardelli, F., Cococcioni, M., 2010. Oil spill classification from multi-spectral satellite images: exploring different machine learning techniques. Proc. SPIE – Int. Soc. Opt. Eng. 7825, 782509.

De Beaucoudrey, N., Schott, P., Bourlier, C., 2003. Detection of oil slicks on sea surface depending on layer thickness and sensor frequency. IGARSS 4, 2741–2743.

De Carolis, G., Adamo, M., Pasquariello, G., 2012. Thickness estimation of marine oil slicks with near-infrared meris and modis imagery: the lebanon oil spill case study. Int. Geosci. Remote Sens. Sympos. (IGARSS) 6350794, 3002–3005.

Denkilkian, H., Koulakezian, A., Ohannessian, R., Chalfoun, M.S., Joujou, M.K.W., Chehab, A., Elhajj, I.H., 2009. Wireless sensor for continuous real-time oil spill thickness and location measurement. IEEE Trans. Instrum. Measur. 58 (12), 4001–4011, art. no. 05291732.

Engdahl, M., Minchella, A., Marinkovic, P., Veci, L., Lu, J., 2012. NEST: an ESA open source toolbox for scientific exploitation of SAR data. Int. Geosci. Remote Sens. Symp. (IGARSS) 6352406, 5322–5324.

Eriksen, P.K., 2013. Leakage and oil spill detection utilizing active acoustic systems. IEEE Int. Underwater Technol. Symp. UT 2013, 6519891.

Etellisi, E.A., Deng, Y., 2012. Oil spill detection: imaging system modeling and advanced image processing using optimized SDC algorithm. Signal, Image Video Proc., 1–15.

Fay, J.A., 1969. The Spread of Oil Slicks on a Calm Sea. Fluid Mechanics Laboratory, Department of Mechanical Engineering, Massachusetts Institute of Technology, Boston, Massachusetts, 14 p.

Ferraro, G., Baschek, B., de Montpellier, G., Njoten, O., Perkovic, M., Vespe, M., 2010. On the SAR derived alert in the detection of oil spills according to the analysis of the EGEMP. Mar. Pollut. Bull. 60 (1), 91–102.

Ferraro, G., Trieschmann, O., Perkovic, M., Tarchi, D., 2012. Confidence levels in the detection of oil spills from satellite imagery: from research to the operational use. Proc. SPIE – Int. Soc. Opt. Eng. 8536, 85360G.

Fingas, M., 2012. How to Measure Oil Thickness (or Not). AMOP, Environment Canada, Ottawa, Ontario, pp. 617–652.

Fingas, M., Brown, C.E., 2011. Oil spill remote sensing: a review. In: Fingas, M. (Ed.), Oil Spill Sci. Techn. Gulf Publishing Company, NY, pp. 111–169 (Chapter 6).

Fingas, M., Brown, C., 2013. Detection of oil in, with and under ice and snow. In: Proceedings of the Thirty-Sixth Arctic and Marine Oil Spill Program Technical Seminar, Environment Canada, Ottawa, Ontario, pp. 472–497.

Gangeskar, R., 2004. Automatic oil-spill detection by marine X-band radars. Sea Technol. 45 (8), 40–45.

Garcia-Pineda, B., MacDonald, I.R., Zimmer, B., 2008. Synthetic aperture radar image processing using the supervised textural-neural network classification algorithms. IGARSS IV (1), IV1265–IV1268, 4779960.

Gens, R., 2008. Oceanographic applications of SAR remote sensing. GISci. Rem. Sens., 275–305.

Gonzalez, C., Sanchez, S., Paz, A., Resano, J., Mozos, D., Plaza, A., 2013. Use of FPGA or GPU-based architectures for remotely sensed hyperspectral image processing, integration. VLSI J. 46 (2), 89–103.

Goodman, R.H., Fingas, M.F., 1988. The use of remote sensing in the determination of dispersant effectiveness. Spill Technol. Newslett. 13 (3), 55–58.

Goodman, R., Bannerman, K., Quintero-Mármol, A.M., Stevenson, G., 2004. Spreading of oil and the concept of average oil thickness. AMOP, 57–71.

Grimaldi, C.S.L., Casciello, D., Coviello, I., Lacava, T., Pergola, N., Tramutoli, V., 2011. An improved RST approach for timely alert and near real time monitoring of oil spill disasters by using AVHRR data. Natural Hazards Earth Syst. Sci. 11 (5), 1281–1291.

Hensley, S., Jones, Lou, Y., 2012. Prospects for operational use of airborne polarimetric SAR for disaster response and management. Int. Geosci. Remote Sens. Sympos. (IGARSS) 6351626, 103–106.

Hoge, F.E., Swift, R.N., 1980. Oil film thickness measurement using airborne laser-induced water raman backscatter. Appl. Opt. 19 (7), 1143–1150.

Hover, G.L., 1994. Testing of infrared sensors for U.S. coast guard oil spill response applications. In: Proceedings of the Second Thematic Conference on Remote Sensing for Marine and Coastal Environments: Needs, Solutions and Applications, ERIM, I, pp. I-47–58.

Hu, C., 2011. An empirical approach to derive MODIS ocean color patterns under severe sun glint. Geophys. Res. Lett. 38 (1), L01603.

Hu, Z., Wei, L., Guo, M., 2012. Method and implementation of oil spill detection in SAR image. Adv. Int. Soft Comput. AISC 133, 753–760.

Hühnerfuss, H., Alpers, W., Witte, F., 1989. Layers of different thicknesses in mineral oil spills detected by grey level textures of real aperture radar images. Int. J. Remote Sens. 10 (6), 1093–1099.

Hühnerfuss, H., Alpers, W., Dannhauer, H., Gade, M., Lange, P.A., Neumann, V., Wismann, V., 1996. Natural and man-made sea slicks in the north sea investigated by a helicopter-borne 5-frequency Radar Scatterometer. Int. J. Rem. Sens. 17 (8), 1567–1582.

Jones, B., 2001. A comparison of visual observations of surface oil with synthetic aperture radar imagery of the sea empress spill. Int. J. Remote Sens. 22, 1619–1638.

Kasilingam, D., 1995. Polarimetric radar signatures of oil slicks for measuring slick thickness. In: Proceedings of Combined Optical-Microwave Earth and Atmospheric Sensing, p. 94.

Kim, D.-J., Moon, W.M., Kim, Y.-S., 2010. Application of TerraSAR-X for emergent oil-spill monitoring. IEEE Trans. Geosci. Remote 48 (2), 852–862.

Kokaly, R.F., Couvillion, B.R., Holloway, J.M., Roberts, D.A., Ustin, S.L., Peterson, S.H., Khanna, S., Piazza, S.C., 2013. Spectroscopic remote sensing of the distribution and persistence of oil from the deepwater horizon spill in barataria bay marshes. Remote Sens. Environ. 129, 210–230.

Kordyban, E., 1982. Oil thickness variation on wavy water in the presence of wind. J. Fluids Trans. 104 (1), 81–87.

Koulakezian, A., Ohannessian, R., Denkilkian, H., Chalfoun, M., Joujou, M.K., Chehab, A., Elhajj, I.H., 2008. Wireless sensor node for real-time thickness measurement and localization of oil spills. In: IEEE/ASME International Conference on Advanced Intelligent Mechatronics, AIM, art. no. 4601733, pp. 631–636.

Kroutil, R.T., Shen, S.S., Lewis, P.E., Miller, D.P., Cardarelli, J., Thomas, M., Curry, T., Kudaraskus, P., 2010. Airborne remote sensing for deepwater horizon oil spill emergency response. Proc. SPIE – Int. Soc. Opt. Eng. 7812, 78120E.

Kudryashova, G.S., Yu, V., Obraztsovm, A.G., Opekan, N.I., Perminov, Protasov, Yu.S., 1986. Optical properties of liquid dielectrics in the ultraviolet, visible, and near infrared regions of the spectrum. J. Appl. Spectrosc. 43 (4), 1108–1113.

Kukhtarev, N., Kukhtareva, T., Gallegos, S.C., 2011. Holographic interferometry of oil films and droplets in water with a single-beam mirror-type scheme. Appl. Opt. 50 (7), B53–B57.

Kuzmanic, I., Vujovic, I., 2010. Oil spill detection in SAR images using wavelets and morphology. In: ELMAR 2010 Proceedings, 5606144, pp. 337–340.

Leifer, I., Clark, R., Jones, C., Holt, B., Svejkovsky, J., Swayse, G., 2011. Satellite and airborne oil spill remote sensing: state of the art and application to the BP deepwater horizon oil spill. AMOP, 270–295.

Leifer, I., Lehr, B., Simecek-Beatty, D., Bradley, E., Clark, R., Dennison, P., Hu, Y., Matheson, S., Jones, C., Holt, B., Roberts, D., Svejkovsky, J., Swayse, G., 2012. State of the art satellite and airborne oil spill remote sensing: application to the bp deepwater horizon oil spill. Remote Sens. Environ. 124, 185–209.

Lennon, M., Babichenko, S., Thomas, N., Mariette, V., Mercier, G., Lipsin, A., 2006. Detection and mapping of oil slicks in the sea by combined use of hyperspectral imagery and laser-induced fluorescence. Proc. EARSel 5, 120–128.

Li, Y., Yu, S., Ma, L., Liu, M., Li, Q., 2008. Satellite image processing and analyzing for marine oil spills. SPIE 7145, 71450C.

Li, Y., Li, J., Zhao, Q., 2011. Microwave remote sensing sea surfaces covered in oil, 2011. In: 2011 International Conference on Electric Information and Control Engineering, ICEICE, paper number 5777670, pp. 2319–2322.

Li, Y., Liu, B.-X., Li, B.-Y., Chen, D., 2012. Analysis of spectral characteristics of oil film on water based on wavelet transform. Guang Pu Xue Yu Guang Pu Fen Xi/ Spectroscopy and Spectral Anal 32 (7), 1923–1927.

Liu, K., Wang, X., 2012. Oil spill in SAR image denoising method based on contourlet HMT. Key Eng. Mater. 500, 545–549.

Liu, P., Zhao, C., Li, X., He, M., Pichel, W., 2010. Identification of ocean oil spills in sar imagery based on fuzzy logic algorithm. Int. J. Rem. Sens. 31 (17), 4819–4833.

Liu, B., Li, Y., Chen, P., Guan, Y., Han, J., Large oil spill surveillance with the use of MODIS and AVHRR images, 2011. In: 2011 International Conference on Remote Sensing, Environment and Transportation Engineering, RSETE 2011 – Proceedings, Paper number 5964523, pp. 1317–1320.

Liu, L., Cui, X., Chen, M., Sun, Y., 2013. Marine oil spill detection in sar image based on mathematical morphology. Appl. Mech. Mater. 256-259 (PART 1), 2320–2323.

Lotliker, A., Mupparthy, R., Kumer, S., Nayak, S., 2008. Evaluation of Hi-resolution MODIS-aqua data for oil spill monitoring. SPIE, 71500S.

Lu, Y., Li, X., Tian, Q., Han, W., 2012. An optical remote sensing model for estimating oil slick thickness based on two-beam interference theory. Opt. Exp. 20 (22), 24496–24504.

Lu, Y., Tian, Q., Wang, X., Zheng, G., Li, X., 2013. Determining oil slick thickness using hyperspectral remote sensing in the Bohai sea of China. Int. J. Digital Earth 6 (1), 76–93.

MacDonald, I.R., Guinasso Jr., N.L., Ackleson, S.G., Amos, J.F., Duckworth, R., Sassen, R., Brooks, J.M., 1993. Natural oil slicks in the gulf of mexico visible from space. J. Geophys. Res. 98 (16), 351–364.

Marghany, M., Hashim, M., 2011. Comparative algorithms for oil spill automatic detection using multimode RADARSAT-1 SAR Data. Int. Geosci. Remote Sens. Symp. (IGARSS) 6049597, 2173–2176.

Martinis, S., Gahler, M., Twele, A., 2012. A multi-scale markov model for unsupervised oil spill detection in TerraSAR-X Data. Int. Geosci. Remote Sens. Sympos. (IGARSS) 6351405, 923–926.

Mastin, G.A., Mason, J.J., Bradley, J.D., Axline, R.M., Hover, G.L., 1994. A comparative evaluation of SAR and SLAR. In: Proceedings of the Second Thematic Conference on Remote Sensing for Marine and Coastal Environments: Needs, Solutions and Applications, ERIM, I, pp. 7–16.

Medialdea, T., Somoza, L., Leon, R., Farran, M., Ercilla, G., et al., 2008. Multibeam backscatter as a tool for sea-floor characterization and identification of oil spills in the galicia bank. Mar. Geol. 249 (01-February), 93–107.

Mera, D., Cotos, J.M., Varela-Pet, J., Garcia-Pineda, O., 2012. Adaptive thresholding algorithm based on SAR images and wind data to segment oil spills along the northwest coast of the Iberian Peninsula. Mar. Pollut. Bull. 64 (10), 2090–2096.

Michel, J., 2011. Submerged oil. In: Fingas, M. (Ed.), Oil Spill Science and Technology. Gulf Publishing Company, NY, NY, pp. 959–981 (Chapter 26).

Migliaccio, M., 2005. A physical approach for the observation of oil spills in SAR images. IEEE J. Oceanic Eng. 30 (3), 496–507.

Migliaccio, M., Ferrara, G., Gambardella, A., Nunziata, F., Sorrentino, A., 2007. A physically consistent stochastic model to observe oil spills and strong scatterers on SLC SAR Images. IGARSS 4423049, 1322–1325.

Migliaccio, M., Nunziata, F., Gambardella, A., 2009. On the co-polarized phase difference for oil spill observation. Int. J. Remote Sens. 30 (6), 1587–1602.

Migliaccio, M., Nunziata, F., Montuori, A., Li, X., Pichel, W.G., 2011. A multifrequency polarimetric SAR processing chain to observe oil fields in the Gulf of Mexico. IEEE Trans. Geosci. Remote Sens. 49 (12 PART 1), 4729–4737 (5958601).

Minchew, B., Jones, C.E., Holt, B., 2012. Polarimetric analysis of backscatter from the deepwater horizon oil spill using l-band synthetic aperture radar. IEEE Trans. Geosci. Remote Sens. 50 (10 PART1), 3812–3830 (6166389).

Mishra, A., Chaudhuri, D., Bhattacharya, C., Rao, Y.S., 2011. Ocean disturbance feature detection from SAR images – an adaptive statistical approach. In: 3rd International Asia-Pacific Conference on Synthetic Aperture Radar, APSAR 2011, (6087017) pp. 163-166.

Morales, D.J., Moctezuma, M., Parmiggiani, F., 2008. Detection of oil slicks in SAR images using hierarchial MRF. IGARSS 3 (1), III1390–III1393 (4779620).

Morinaga, T., Arakawa, H., Shouji, M., Kiyomiya, T., 2003. Estimate of the slick thickness for leaked heavy oil from the sunken Nakhodka in the sea of Japan. Mer 41 (2-3), 114–121.

Muellenhoff, O., Bulgarelli, B., Ferraro, G., Topouzelis, K., 2008. The use of ancillary metocean data for the oil spill probability assessment in SAR images. Fresenius Environ. Bull. 17 (9B), 1383–1390.

Myasoedov, A., Johannessen, J.A., Kudryavtsev, V., Collard, F., Chapron, B., 2012. Sun glitter as a "tool" for monitoring the ocean from space. In: 2nd International Conference on Remote Sensing, Environment and Transportation Engineering, RSETE 2012 – Proceedings, 6260759.

Nie, W., Zhang, X., 2012. Detecting marine oil spill pollution based on borda count method of ocean water surface image. In: 2nd International Conference on Remote Sensing, Environment and Transportation Engineering, RSETE 2012 – Proceedings, 6260531.

Nøst, E., Egset, C.N., 2006. Oil spill detection system – results from field trials. Proc. Oceans Mar. Technol. Soc., art. no. 4099060.

Nunziata, F., Migliaccio, M., Sobieski, P., 2008. A BPM two-scale contrast model. IGARSS IV, 593596.

Nunziata, F., Gambardella, A., Migliaccio, M., 2012. A unitary mueller-based view of polarimetric SAR oil slick observation. Int. J. Remote Sens. 33 (20), 6403–6425.

Nunziata, F., Gambardella, A., Migliaccio, M., 2013. On the degree of polarization for SAR sea oil slick observation. ISPRS J. Photogramm. Remote Sens. 78, 41–49.

O'Hara, P.D., Serra-Sogas, N., Canessa, R., Keller, P., Pelot, R., 2013. Estimating discharge rates of oily wastes and deterrence based on aerial surveillance data collected in Western Canadian marine waters. Mar. Pollut. Bull. 69 (01-February), 157–164.

O'Neil, R.A., Neville, R.A., Thompson, V., 1983. The arctic marine oilspill program (AMOP) remote sensing study, Environment Canada Report EPS 4-EC-83-3.

Otremba, Z., Piskozub, J., 2001. Modelling of the optical contrast of an oil film on a sea surface. Opt. Exp., 411–416.

Ozkan, C., Ozturk, C., Sunar, F., Karaboga, D., 2011. The artificial bee colony algorithm in training artificial neural network for oil spill detection. Neural Network World 21 (6), 473–492.

Patsayeva, S., Yuzhakov, V., Valamov, V., Barbina, R., Fantoni, R., Frassanito, C., Palucci, A., 2000. Laser spectroscopy of mineral oils on the water surface. Proceedings of EARSel Workshop LIDAR.

Pelyushenko, S.A., 1993. Microwave radiometer system for the detection of oil slicks. Oil Spill Sci. Technol. 2, 249–254.

Pfeifer, C., Brzozowski, E., Markian, R., Redman, R., 2008. Quantifying percent cover of submerged oil using underwater video imagery. IOSC, 269–278.

Pinel, N., Bourlier, C., 2009. Unpolarized infrared emissivity of oil films on sea surfaces. IGARSS 2 (2), II85–II88 (5418007).

Piskozub, J., Drozdowska, V., Varlamov, V., Lidar, A., 1997. System for remote measurement of oil film thickness on sea surface. In: Proceedings of the Fourth Thematic Conference on Remote Sensing for Marine and Coastal Environments, ERIM, pp. I386–I392.

Rand, R.S., Clark, R.N., Livo, K.E., 2011. Feature-based and statistical methods for analysing the deepwater horizon oil spill with AVIRIS imagery. Proc. SPIE – Int. Soc. Opt. Eng. 8158, 81580N.

Reimer, E.R., Rossiter, J.R., 1987. Measurement of oil thickness on water from aircraft; A. Active microwave spectroscopy; B: Electromagnetic Thermoelastic Emission, Environmental Studies Revolving Fund, Report Number 078.

Robbe, N., Hengstermann, T., 2006. Remote sensing of marine oil spills from airborne platforms using multi-sensor systems. Water Pollut. VIII: Model. Monit. Manage., 347–355.

Robson, M., Secker, J., Vachon, P.W., 2006. Evaluation of ecognition for assisted target detection and recognition in SAR imagery. IGARSS 1454241189, 145–148.

Salberg, A.-B., Rudjord, O., Solberg, A.H.S., 2012. Model based oil spill detection using polarimetric SAR. Int. Geosci. Remote Sens. Sympos. (IGARSS) 6352270, 5884–5887.

Salisbury, J.W., D'Aria, D.M., Sabins, F.F., 1993. Thermal infrared remote sensing of crude oil slicks. Remote Sens. Environ. 45 (2), 225–231.

Sarma, A.K., Ryder, A.G., 2006. Comparison of the fluorescence behaviour of a biocrude oil and crude petroleum oils. Energy Fuels 20 (2), 783–785.

Shen, H.-Y., Zhou, P.-C., Feng, S.-R., 2011. Research on multi-angle near infrared spectral-polarimetric characteristic for polluted water by spilled oil. Proc. SPIE – Int. Soc. Opt. Eng. 8193, 81930M.

Shi, L., Ivanov, A.Y., He, M., Zhao, C., 2008. Oil spill mapping in the western part of the east china sea using synthetic aperture radar imagery. Int. J. Remote Sens. 29 (21), 6315–6329.

Shih, W.-C., Andrews, A.B., 2008a. Infrared contrast of crude-oil-covered water surfaces. Opt. Lett. 33 (24), 3019–3021.

Shih, W.-C., Andrews, A.B., 2008b. Modeling of thickness dependent thermal contrast of native and crude oil covered water surfaces. Opt. Exp. 16 (14), 10535–10542.

Shu, Y., Li, J., Yousef, H., Gomes, G., 2010. Dark-spot detection from SAR intensity imagery with spatial density thresholding for oil-spill monitoring. Remote Sens. Environ. 114 (9), 2026–2035.

Singha, S., Bellerby, T.J., Trieschmann, O., 2012. Detection and classification of oil spill and look-alike spots from SAR imagery using an artificial neural network. Int. Geosci. Remote Sens. Sympos. (IGARSS) 6352042, 5630–5633.

Singha, S., Bellerby, T.J., Trieschmann, O., 2013. Satellite oil spill detection using artificial neural networks. IEEE J. Select. Topics Appl. Earth Observ. Remote Sens. (in press).

Sipelgas, L., Uiboupin, R., 2007. Elimination of oil spill like structures from radar image using MODIS data. IGARSS 4422822, 429–431.

Skou, N., Toselli, F., Wadsworth, A., 1983. Passive radiometry and other remote sensing data interpretation for oil slick thickness assessment, in an experimental case (Mediterranean Sea). In: Proc. EARSeL/ESA Symposium on Remote Sensing Applications for Environmental Studies, Brussels, pp. 211–216.

Skrunes, S., Brekke, C., Eltoft, T., 2012. Oil spill characterization with multi-polarization C- and X-band SAR. Int. Geosci. Remote Sens. Symp. (IGARSS) 6352459, 5117–5120.

Solberg, A.H.S., 2012. Remote sensing of ocean oil-spill pollution. Proc. IEEE 100 (10), 2931–2945 (6235983).

Solberg, R., Theophilopoulos, N., 1997. ENVISYS – a solution for automatic oil spill detection in the mediterranean. In: Proceedings of the Fourth Thematic Conference on Remote Sensing for Marine and Coastal Environments, ERIM, pp. I-3-11-8.

Sumimoto, T., Okada, S., Imade, M., Ohta, M., 1986. Measurement of spilled oil thickness with an ultrasonic gauging apparatus. J. Sound Vib. 111 (2), 352–356.

Sun, Z.-Q., Zhao, Y.-S., Yan, G.-Q., Li, S.-P., 2011. Study on the hyperspectral polarized reflection characteristics of oil slicks on sea surfaces. Chinese Sci. Bull. 56, 1596–1603.

Sun, M., Shi, C., Li, H., 2013. Comparison operator edge detection based on remote sensing of marine oil spill. Adv. Mater. Res. 610–613, 3747–3751.

Suo, Y.-F., Chi, T., Ling, P., 2012. Review on the key technology of real-time oil spill monitoring system based on marine radar. In: 2nd International Conference on Remote Sensing, Environment and Transportation Engineering, RSETE 2012 – Proceedings, 6260717.

Svejkovsky, J., Muskat, J., 2006. Real time detection of oil slick thickness patterns with a portable multispectral scanner, Report to U.S. DOE, MMS.

Svejkovsky, J., Muskat, J., Mullin, J., 2008. Mapping oil slick thickness patterns with a portable multispectral aerial imager. IOSC.

Svejkovsky, J., Lehr, W., Muskat, J., Graettinger, G., Mullin, J., 2012. Operational utilization of aerial multispectral remote sensing during oil spill response: lessons learned during the deepwater horizon (MC-252) spill. Photogramm. Eng. Remote Sens. 78 (10), 1089–1102.

Taylor, S., 1992. 0.45 to 1.1 μm spectra of prudhoe crude oil and of beach materials in prince william sound, Alaska, CRREL Special, Report No. 92–5.

Tebeau, P.A., Hansen, K.A., Fant, J.W., Terrien, M.M., 2007. Assessing the long-term implementation costs versus benefits associated with laser fluorosensor spill response technology. AMOP, 451–460.

Tello, M., Bonastre, R., Lopez-Martinez, C., Mallorqui, J.J., Danisi, A., 2007. Characterization of local regularity in SAR imagery by means of multiscale techniques: application to oil spill detection. IGARSS, 5228.

Tian, W., Shao, Y., Wang, S., 2008. A system for automatic identification of oil spill in ENVISAT ASAR. Int. Geosci. Remote Sens. Symp. (IGARSS) 4779621, 394–397.

Topouzelis, K., Psyllos, A., 2012. Oil spill feature selection and classification using decision tree forest on SAR image data. ISPRS J. Photogramm. Remote Sens. 68 (1), 135–143.

Topouzelis, K., Karanthanassi, V., Pavlakis, P., Rokos, D., 2007. Detection and discrimination between oil spills and look-alike phenomena through neural networks. ISPRS J. Photogramm. Remote Sens. 62 (4), 264–270.

Topouzelis, K., Karanthanassi, V., Pavlakis, P., Rokos, D., 2008. Dark formation detection using neural networks. Int. J. Remote Sens. 29 (16), 4705–4720.

Topouzelis, K., Stathakis, D., Karanthanassi, V., 2009a. Investigation of genetic contribution to feature selection for oil spill detection. Int. J. Remote Sens. 30 (3), 611–625.

Topouzelis, K., Karanthanassi, V., Pavlakis, P., Rokos, D., 2009b. Potentiality of feed-forward neural networks for classifying dark formation to oil spills and look-alikes. Geocarto Int. 24 (3), 179–191.

True, M., Shuchman, R., Kletzli, D.W., Johannessen, J.A., Digranes, G., Berg, S., Dalland, K., 1994. Thickness characterisation of oil spills using active microwave sensors. Proce. SPIE – Int. Soc. Opt. Eng. 2319, 92–103.

Ulaby, F.T., Moore, R.K., Fung, A.K., 1989. Microwave remote sensing: active and passive. Artech House, 1466–1479.

Vespe, M., Greidanus, H., 2012. SAR image quality assessment and indicators for vessel and oil spill detection. IEEE Trans. Geosci. Remote Sens. 50 (11 PART2), 4726–4734.

Vespe, M., Ferraro, G., Posada, M., Greidanus, H., Perkovic, M., 2011. Oil spill detection using COSMO-skymed over the adriatic sea: the operational potential. Int. Geosci. Remote Sens. Symp. (IGARSS) 6050208, 4403–4406.

Viser, T., 1979. Teledetection of the thickness of oil films on polluted water based on the oil fluorescence properties. Appl. Opt., 1746–1749.

Wang, D., Pan, D., Zhan, Y., Zhu, Q., 2010a. Experiment of monitoring oil spill on the base of EOS/MODIS data. Proc. SPIE – Int. Soc. Opt. Eng. 7831, 78311T.

Wang, D., Gong, F., Pan, D., Hao, Z., Zhu, Q., 2010b. Introduction to the airborne marine surveillance platform and its application to water quality monitoring in China. Oceanol. Sin., 33–39.

Weber, T.C., De Robertis, A., Greenaway, S.F., Smith, S., Mayer, L., Rice, G., 2012. estimating oil concentration and flow rate with calibrated vessel-mounted acoustic echo sounders. Proc. Natl. Acad. Sci. USA 109 (50), 20240–20245.

Wendelboe, G., Fonseca, L., Ericksen, M., Hvidbak, F., Mutschler, M., 2009. Detection of heavy oil on the seabed by application of a 400 kHz multibeam echo sounder. AMOP, 791–806.

Wettle, M., Daniel, P.J., Logan, G.A., Thankappan, M., 2010. Assessing the effect of hydrocarbon type and thickness on a remote sensing signal: a sensitivity study based on the optical properties of two different oil types and the HYMAP and quickbird sensors. Remote Sens. Environ. 113 (9), 2000–2010.

Xiao, J.-W., Tian, Q.-J., 2012. Experimental study of offshore oil thickness hyperspectral inversion based on bio-optical model. Guang Pu Xue Yu Guang Pu Fen Xi/Spectroscopy Spectral Anal. 32 (1), 183–187.

Yang, C.-S., Kim, Y.-S., Ouchi, K., Na, J.-H., 2009. Comparison with L-, C-, and X-band real SAR images and simulation SAR images of spilled oil on sea surface. IGARSS IV, 673–676.

Yin, D., Huang, X., Qian, W., Huang, X., Li, Y., Feng, Q., 2010. Airborne validation of a new-style ultraviolet push-broom camera for ocean oil spill pollution surveillance. Proc. SPIE 7825, 738403.

Yin, Q.-Z., Li, K., Zhou, C., Liu, C., Chu, X.-M.., Zheng, J., 2012. Research on oil spill monitoring experiments based on OFD-1 oil film detector. In: 2012 2nd International Conference on Remote Sensing, Environment and Transportation Engineering, RSETE 2012 – Proceedings, 6260699.

Yuan, Y., Fang, Y., Cui, F., Li, D., 2011. Research on preprocessing algorithm for differential polarization spectrum of oil spills on water. Guangxue Xuebao/Acta Opt. Sinica 31 (11), 1128001-1–1128001-7.

Yujiri, L., Shoucri, M., Moffa, P., 2003. Passive millimeter wave imaging. IEEE Microwave Mag. 4 (3), 39–50.

Zhan, Y., Mao, T., Gong, F., Wang, D., Chen, J., 2010. An oil film information retrieval method overcoming the influence of sun glitter – based on AISA+ airborne hyper-spectral image. Proc. SPIE 7825, 78925m.

Zhang, F., Shao, Y., Tian, W., Wang, S., 2008. Oil spill identification based on textural information of SAR image. IGARSS IV (1308).

Zhang, Y., Li, H., Wang, X., Dan, W., 2010. Edge extraction of marine oil spill in SAR images. In: International Conference on Challenges in Environmental Science and Computer Engineering, CESCE, Paper number, 5493170, pp. 439–442.

Zhang, Y., Lin, H., Lium, Q., Hu, J., Li, X., Yeung, K., 2012. Oil-spill monitoring in the coastal waters of Hong Kong and Vicinity. Mar. Geodesy 35 (1), 93–106.